

Acoustic Transfer Matrix Reconstruction and Analysis for Ducts with Sudden Change of Area

Alexander M.G. Gentemann, Andreas Fischer, Stéphanie Evesque, Wolfgang Polifke

Technische Universität München, Munich, Germany

Abstract

In many fields of application, the acoustic properties of fluid machinery are of growing importance. To determine these properties, it is often a reasonable approximation to model a complex geometry as a network of acoustic elements. Acoustic elements can be characterized by their transfer matrices. An acoustic transfer matrix describes the transformation of the acoustic field variables by an acoustic element as a function of frequency. It is a quantitative assessment for the modification of the acoustic wave characteristics.

This paper describes a procedure for the estimation of acoustic transfer matrices by means of computational fluid dynamics (CFD). A transient solution of the Navier-Stokes equations is performed, using a compressible, low Mach-number RANS scheme with broad band excitation of the flow variables at the boundaries. On the basis of the resulting time series for pressure and velocity, the transfer matrix for an acoustic element is estimated by application of a system identification procedure based on the Wiener-Hopf equation.

Sudden changes in cross section of ducts are very common in acoustic designs, e.g. in mufflers or combustion chambers. Therefore, the transfer matrix of this element is important for the design of flow systems involving acoustics. The sudden change in cross sectional area between two pipes is used as a test case for the CFD-based estimation method for acoustic transfer matrices. The method is validated against experimental data, finite element calculations, as well as an analytical description.

1. Introduction

The acoustic analysis of flow systems is important for the design process in many fields of application. The propagation of acoustic perturbations through the system or the possibility of system instabilities might be of interest. The design of gas turbine combustors is one important field of application. With the implementation of premixed combustion to reduce NOx emission, the susceptibility of the designs to thermo-acoustic instabilities increases greatly. These instabilities can cause mechanical damage of the combustor¹⁹.

Different approaches to the subject are possible. The separation of an acoustic system into

parts, the acoustic elements, is one possibility, where the system is separated into functional elements, e.g. pipes, area changes, a flame, etc. This approach offers many advantages, e.g. it is easy to analyze quickly different configurations in the design process.

For this approach, information about the acoustic elements is required. Acoustic elements can be characterized by their transfer matrices, which describe the transformation of the acoustic field variables by an acoustic element as a function of frequency

$$\begin{pmatrix} \frac{p'}{\rho c} \\ u' \end{pmatrix}_d = \hat{T}(\omega) \begin{pmatrix} \frac{p'}{\rho c} \\ u' \end{pmatrix}_u, \quad (1)$$

where u and d refer to the locations up- and downstream of the acoustic element, \hat{T} represents the transfer matrix of the element. Eq. (1) is shown in (pu) notation, which means the matrix connects the primitive acoustic variables, pressure and velocity. The transfer matrix can also be the connecting element between the acoustic waves. This wave representation is achieved by the (fg) and scattering (sr) notations. Both of these transfer matrix notations connect upstream (f) and downstream (g) traveling waves. For (sr) notation, waves traveling towards the element (f_u, g_d) are signals, waves traveling away are responses (f_d, g_u). For (fg) notation, the upstream waves are signals (f_u, g_u), the downstream waves are responses (f_d, g_d). In principle, all three transfer matrix notations are equivalent. But for the transfer matrix estimation procedure, the choice of notation becomes important.

A method to determine acoustic transfer matrices is needed, which incorporates the effects of mean flow, turbulence, and combustion. In this paper, computational fluid mechanics (CFD) serves as the basis for the estimation of acoustic transfer matrices. A transient CFD calculation is combined with excitation of flow variables on both boundaries¹. At defined planes inside the computational domain, values for pressure and velocity are exported to files at every time step. These time series are imported into an external post processor to apply the Wiener-Hopf system identification method, which is used to extract the acoustic transfer matrix. The combination of CFD and the post processor will be referred to as CFD/SI.

The sudden change of cross sectional area between two ducts is a test case to validate this method

against experiment, finite element acoustic analysis, and analytical results. The sudden area change is very common in combustor designs and its transfer matrix is therefore important.

First, the general CFD-based estimation method for acoustic transfer matrices is described. Then, the experimental setup, the finite element method (FEM), and the analytic representation for sudden area changes are introduced. Finally, results obtained from the four methods (CFD/SI, FEM, analytic, experiment) are compared and analyzed.

2. Transfer Matrix Reconstruction from CFD Calculation

The transfer matrix reconstruction procedure is a combination of computational fluid dynamics (CFD) and a post processor. CFD is used to compute time series of pressure and velocity, which are correlated in the post processor to estimate the acoustic transfer matrix.

The application of CFD/SI for the estimation of acoustic transfer matrices was introduced by Polifke at al.^{1,2}. A system identification procedure was used for comparison between analytical flame transfer matrices to CFD results. Zhu at al.³ adopted the method for comparison of flame transfer functions in a liquid fuel combustor. Response filters were used to estimate the flame transfer function. Polifke at al. applied response filters to flame transfer function estimation by means of stationary CFD⁴.

2.1 General Procedure

Fig. 1 shows the setup of a CFD calculation in generalized form. *bc* indicates the boundary conditions of the computational domain. Mean flow enters from the left. The flow field is excited on both boundaries by addition of velocity (inlet boundary) and pressure (outlet boundary) fluctuations to the mean values:

$$u_{inlet}(t) = \bar{u} + u'_{in}(t) \quad , \quad (2)$$

$$p_{outlet}(t) = \bar{p} + p'_{out}(t) \quad . \quad (3)$$

This results in waves traveling towards the "black box" represented by the transfer matrix T (eq. (1)). Once the waves reach the boundaries, they are partially reflected and transmitted. This is depicted by the smaller arrows with dotted lines. At locations up- and downstream of the acoustic element in question, time series for pressure and velocity are extracted and written to files. Δx refers to the axial distance between the monitoring locations.

The acoustic post processor is the second module necessary to estimate transfer matrices from CFD. It imports the time series created with the CFD code. After static pressure and axial velocity are imported, the respective average values are subtracted

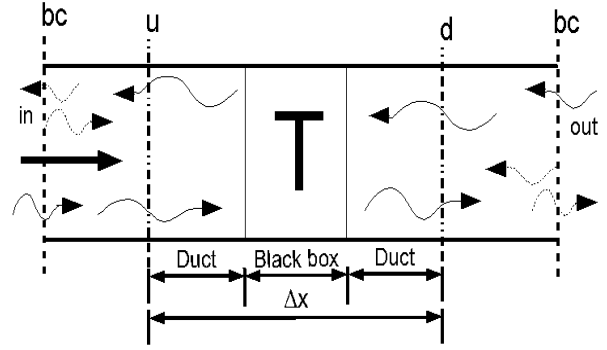


Fig. 1 CFD Setup and Acoustic Element.

to obtain p' and u' . Then, Riemann invariants for plane wave propagation are calculated to represent the up- and downstream waves:

$$f = \frac{1}{2} \left(\frac{p'}{\rho c} + u' \right) \quad g = \frac{1}{2} \left(\frac{p'}{\rho c} - u' \right) \quad . \quad (4)$$

The Wiener-Hopf equation, a system identification procedure known from control theory, is applied for the purpose of the transfer matrix estimation⁸:

$$\left(\frac{1}{N-L+1} \sum_{i=L}^N s_{l-i} s_{l-j} \right) h_i = \left(\frac{1}{N-L+1} \sum_{l=L}^N s_{l-i} r_l \right) \quad . \quad (5)$$

In eq. (5), N is the number of time steps, L the length of the unit impulse response (the order of the filter), s is the signal, r the response, and h is the unit impulse response, which is to be estimated, i and j run from 0 to $L-1$. A more complete description is given elsewhere^{2,8,9}.

The term in brackets on the left side of eq.(5) approximates the autocorrelation matrix of the signals, the term in brackets on the right side of eq. (5) approximates the crosscorrelation vectors of signals and responses, and h is computed by inversion of eq. (5). The unit impulse response h is then z-transformed to obtain the transfer matrix⁹. The estimated transfer matrix mathematically represents the sum of all acoustic elements located between the export locations (ref. Fig. 1). In the case depicted in fig 1, this means three elements: 2 ducts and the element under consideration. Since the transfer matrix for plane wave propagation is known from first principles, the acoustic elements are separated to estimate the transfer matrix of the desired element.

2.2 Specific Issues

The boundary conditions present an important aspect of the CFD setup. The standard 'velocity inlet' and 'pressure outlet' boundary conditions, available in most CFD codes, maintain high reflection coefficients.

This, external forcing, and the frequency response of the system can cause resonance peaks. The system would then be signal invariant, which makes it impossible to estimate acoustic transfer matrices^{6,7}.

The preferred solution to the problem is a boundary condition with low (ideally zero) reflection coefficient⁷. This feature is not available for the CFD code used. A “work around” for the problem is the use of the existing velocity inlet and pressure outlet boundary conditions and the application of white noise as the perturbation on both boundaries. A system excited with white noise on just one boundary shows resonance peaks. Once both boundaries are excited this way, the magnitude of the resonance peaks decreases. The reason for this is the stochastic fluctuation of the flow variables at the boundaries. The stochastic fluctuations from one boundary meet a stochastically fluctuating second boundary and vice versa. This suppresses resonant excitation.

A perturbation magnitude of 10% of the mean value is used:

$$u'_{in}(t) = 0.1 \bar{u}_{inlet} X_{fluc}^{inlet}(t) , \quad (6)$$

$$p'_{out}(t) = 0.1 \rho \bar{u}_{outlet}^2 X_{fluc}^{outlet}(t) , \quad (7)$$

where X_{fluc} is white noise between -0.5 and 0.5. For further use in the post processor, mass averaged values for static pressure and axial velocity are extracted.

The variable L , the number of coefficients of the unit impulse response vector, is a free parameter in the identification process. A minimum value is found, for acoustic systems with low Mach number flow, by considering the time a disturbance needs to travel through the element. Therefore,

$$L_{min} \approx \frac{\Delta x}{\bar{c} \Delta t} , \quad (8)$$

where Δx is the axial distance between the two data export locations, denoted in fig. 1, and Δt is the time step of the CFD calculation.

The value chosen for L needs to be larger than L_{min} . The reason for this, among others, is that the time-lag of the black box may be located between two time steps¹⁸. But the value for L_{min} has to be of the same order of magnitude to avoid numerical inaccuracy⁹.

The time series imported, and thus the resulting signals and responses, are limited in frequency content. Time step Δt and maximum computation length $N\Delta t$ determine the minimum and maximum frequency associated with the data. ω_{min} and ω_{max} are computed as

$$\omega_{min} = \frac{1}{T_{max}} \quad \omega_{max} = \frac{1}{2\Delta t} , \quad (9)$$

where T_{max} denotes the computation length. ω_{max} is also known as the Nyquist frequency¹⁸.

2.3 Application of the Method to Sudden Area Changes

In the following, the sudden change of cross sectional area between two pipes will serve as a test case. The setup, used for this study, includes turbulent flow without heat release.

Fluid Model	Ideal Gas Law
Turbulence Model	Standard k-ε
Discretization	SIMPLE Method
Advection Scheme	Power Law
Time Step dt [sec]	$2.5 \cdot 10^{-5}$
Time Steps (N)	10000
Mean Temperature [K]	293
Mach Number	< 0.1

Table 1 Setup and Models used for CFD Calculations.

The CFD setup consists of a 2D grid with 500 to 3000 cells and a total length of 0.8m. The transient flow field is computed with the commercial CFD package Fluent 6⁵. Table 1 shows the applied models. Inlet velocity and pressure outlet are used as boundary conditions.

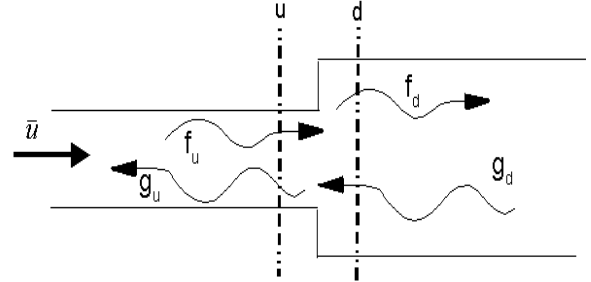


Fig. 2 Area Change and Wave Propagation.

Fig. 2 shows the propagation of waves inside the tube, the arrow on the left indicates the flow direction. Since the Wiener-Hopf system identification method, as shown in eq. (5), is only valid for causal systems, a proper setup of signals and responses is necessary. I.e. incoming waves are considered as “signals”, outgoing waves are “responses” in the system identification procedure. A more complete investigation of the topic of causality is given elsewhere¹⁸. As seen in fig. 3, f at upstream location and g at the downstream location of the acoustic element are treated as signals, f downstream and g upstream are responses. This is referred to as scattering notation (sr):

A criterion for the choice of Δt is currently under investigation. Introducing N and dt into eqs. 9, the resulting frequency boundaries are $\omega_{min} = 25s^{-1}$ and $\omega_{max} = 125663s^{-1}$.



Fig. 3 Signal and Response Formulations as used in System Identification Process.

Since time series are exported at planes 0.05m up- and downstream of the area discontinuity, Δx was 0.1m, the speed of sound is about 343m/s. This results in a minimum value of L , the length of the unit impulse response, of 12. L is chosen to be 17, the value was observed to be the minimum with the same quality of the estimated transfer matrix¹⁸.

In conclusion, the described method provides a procedure to estimate the transfer matrix of acoustic elements including viscous and mean flow effects for arbitrary acoustic elements from CFD calculations. The method, based on the work by Polifke et al.², is improved by application of white noise excitation on the boundaries and the scattering notation for the system identification process. Also, an estimation procedure for the variable L is provided.

3. Other Methods for the Determination of the Transfer Matrix of a Sudden Change of Area

3.1 Experimental Setup

The measurement of acoustic transfer matrices, introduced in this section, is based on an idea proposed by Åbom et al.¹⁰. To measure the acoustic four pole of a test element, pressure and velocity are needed at the desired location. Unfortunately, microphones are only sensitive to pressure. Nevertheless it is possible to calculate pressure and velocity at a position, when the measurements of two microphones connected by an element with known transfer matrix, e.g. a tube, are combined. Using two microphones up- two microphones downstream, respectively, it is possible to evaluate the transfer matrix of any test element.

Experiments showed that the method works in principle, but is sensitive to errors introduced by flow noise. Paschereit et al. expanded the method to an arbitrary number of microphones¹¹. Introducing a larger number of microphones and averaging over multiple measurements, as lined out below, significantly increases the stability of the method as well as its accuracy.

The experimental setup consisted of two pipes of different diameter with solid steel walls joined with a PVC flange. During the experiments, air is blown through the system at a constant rate of 29 g/sec. Sirens attached up- and downstream of the test element allow a

strong excitation on a single frequency through modulation of the siren air mass flow. The sirens are equipped with an optical sensor that allow continuous validation of the excitation frequency during the experiment. For the transfer matrix evaluation, time series of the sensor signal and acoustic pressure at eight positions (four microphones up- and downstream of the test element, respectively) are measured with calibrated microphones.

The signals are recorded simultaneously using a multichannel sample-and-hold board connected to a standard PC system. The time series of the pressure and sensor signals are then Fourier transformed. Only the transformed vectors at the siren excitation frequency are recorded to disk. Subtracting the phase of the siren sensor signal, it is possible to average over a large number of microphone pressure vectors at a single excitation frequency.

For each excitation frequency, 150 independent one-second time series at a sampling rate of 10 kHz are taken and averaged. After amplitude and phase of the pressure at the microphone positions is measured with sufficient accuracy, invariant travelling wave solutions are fitted to the data applying a nonlinear Levenberg-Marquardt algorithm. From this fit, values for the Riemann invariants f and g at the definition plane of the transfer matrix are obtained. For the case of the acoustic transfer matrix of sudden changes of area between two axisymmetric ducts, this position is naturally located at the discontinuity.

Taking the results for two independent measurements with up- and downstream excitation, respectively, a system of linear equations can be set up, which is solved for the transfer matrix elements in (fg) notation

$$\begin{pmatrix} f_u^a & g_u^a & 0 & 0 \\ 0 & 0 & f_u^a & g_u^a \\ f_u^b & g_u^b & 0 & 0 \\ 0 & 0 & f_u^b & g_u^b \end{pmatrix} \begin{pmatrix} T_{11}^{fg} \\ T_{12}^{fg} \\ T_{21}^{fg} \\ T_{22}^{fg} \end{pmatrix} = \begin{pmatrix} f_d^a \\ g_d^a \\ f_d^b \\ g_d^b \end{pmatrix} \quad (10)$$

Via matrix transformation, the transfer matrix is then converted into (pu) notation. For the measurement presented here, the transfer matrix is evaluated at frequency steps of 20 Hz up to a frequency of 1 kHz. More detail is presented by Paschereit et al.¹¹

3.2 Finite Element Computation

The finite element approach, for validation of the CFD/SI transfer matrix estimation method, is based on an FEM acoustic code, which provides the pressure field inside the computational domain. The finite element based approach for determining transfer matrices is formulated as the frequency domain

equivalent to the experimental multi-microphone method introduced above¹². The difference to the measurement procedure is that the propagation of acoustic waves inside the computational domain is obtained by means of finite element calculation.

Since the Helmholtz equation is chosen for the solution process, mean flow, turbulence effects, and combustion are not included in the computation.

The acoustic pressure is recorded at two locations far upstream and two locations far downstream of the acoustic element. Between the two recording positions on each side of the acoustic element, the transfer matrices for plane wave propagation is known. On the basis of this, the acoustic velocity is computed. Then, the acoustic pressures and velocities are extrapolated up to the plane of area change.

To obtain the transfer matrix across a certain frequency range, two calculations are necessary for every frequency in question. Then, it is solved for the transfer matrix by performing two independent calculations, incorporating up- and downstream excitation. A more detailed description is presented by Pankewitz et al.¹².

3.3 Theory

Analytic models for compact acoustic elements can be derived from first principles using the Navier-Stokes and continuity equations. This section is separated into two parts: a.) the derivation of a general form of the transfer matrix for compact elements ($kL \ll 1$), and b.) the determination of the unknown parameters.

3.3.1 Derivation of Acoustic Transfer Matrix for a Compact Element:

To derive a transfer matrix for low Mach number flow and plane wave acoustics, the following form of mass conservation and Bernoulli equations are used (the derivation is found in Appendix A)

$$\left[A \left(\frac{p'}{\rho c} M + u' \right) \right]_u^d + i \frac{\omega}{c} l_{red} A_d \frac{p_u'}{\rho c} = 0 \quad , \quad (11)$$

$$\left[\frac{p'}{\rho c} + M u' \right]_u^d + l_{eff} \frac{i \omega}{c} u_u' + \zeta M_u u_u' = 0 \quad , \quad (12)$$

where p' and u' represent the acoustic pressure and velocity, M is the Mach number, c the speed of sound, ρ the density, and ω the angular frequency. In eq. (11), the term containing l_{red} represents capacitance effects. Generally, l_{red} is defined as

$$l_{red} \equiv \int_{x_u}^{x_d} \frac{A(x)}{A_d} dx \quad , \quad (13)$$

where x refers to the axial position, and A is the cross sectional area. For some elements, for example the sudden change of cross sectional area, the axial locations are hard to define because both locations are equal and the integral vanishes. In eq. (12), ζ represents the acoustic loss over the element, u and d referring to the up- and downstream locations. In analogy to eq. (13), l_{eff} is defined

$$l_{eff} \equiv \int_{x_u}^{x_d} \frac{A_u}{A(x)} dx + l_{ec} \quad , \quad (14)$$

where l_{ec} is the end correction length due to sharp corners. The integral term accounts for the inductance effects of the area discontinuity as mentioned by Munjal¹³.

Eqs. 11 and 12 can easily be transformed into transfer matrix notation with terms of 2nd order in small quantities M or kl being neglected:

$$\hat{T} = \begin{pmatrix} 1 & \left[1 - \zeta - \left(\frac{A_u}{A_d} \right)^2 \right] M_u - i \frac{\omega}{c} l_{eff} \\ -i \frac{\omega}{c} l_{red} - M_d & \frac{A_u}{A_d} \end{pmatrix} \quad . \quad (15)$$

3.3.2 Determination of Parameter Values:

As mentioned above, the axial positions x_u and x_d , needed in eqs. (13) and (14), are difficult to define for a sudden change of area between two rectangular channels. Thus, l_{eff} and l_{red} can not be determined directly from eqs. (13) and (14).

A sudden change of area between two channels can be transformed to a streamline coordinate system by applying the Schwartz-Christoffel transformation¹⁶. After that, the complete acoustic flow field in the two channels can be calculated. By integration of the kinetic energy inside the ducts, the analogous inductance L_a for area contractions and expansions is derived¹⁴

$$L_a = \frac{\rho}{\pi z} \left[\frac{(d_d - d_u)^2}{2 d_u d_d} \ln \frac{d_u + d_d}{|d_d - d_u|} + \ln \frac{(d_u + d_d)^2}{4 d_u d_d} \right] \quad , \quad (16)$$

where z is the channel depth, set to unity for the case of infinity, and d are the diameters of the channels. The geometry discussed in this paper was axisymmetric, whereas the theory by Morse and Ingard (leading to eq. (16)) is for rectangular channels. For small area ratios, the expression can be used for axisymmetric configurations with good accuracy. The depth z is then

set to $0.5d_u$.

l_{eff} is then calculated using the following relation

$$l_{eff} = \frac{L_a A_u}{\rho} \quad , \quad (17)$$

the reduced length can be calculated from L_a as follows¹⁴

$$l_{red} = -\frac{\rho}{L_a c} \quad . \quad (18)$$

The complete derivation of eqs. (17) and (18) is given in Appendix B.

The acoustic power lost across the element is the starting point for the derivation of the analogous resistance R_a for the sudden change of cross sectional area of rectangular channels

$$R_a = \frac{\rho \omega d_v |d_d - d_u|}{2 d_d z} \frac{1}{d_u} \left(1 + \frac{|d_d^2 - d_u^2|}{\pi d_u d_d} \ln \frac{d_u + d_d}{|d_d - d_u|} \right) \quad , \quad (19)$$

$$d_v = \sqrt{\frac{2 \mu \nu}{\rho \omega}}$$

where d_v is the viscous boundary layer thickness¹⁴. The extension to axisymmetric geometries is analogue to L_a .

The acoustic loss coefficient ζ is related to the analogous resistance by the following expression (see Appendix B for details)

$$\zeta = \frac{R_a A_u}{\rho c M_u} \quad . \quad (20)$$

In the following, the analytic expression of the transfer matrix, for the case of pipes, is validated. This is done by comparing the computed analytical transfer matrices to the matrices estimated by means of finite element (FEM) calculations, which have proven to show

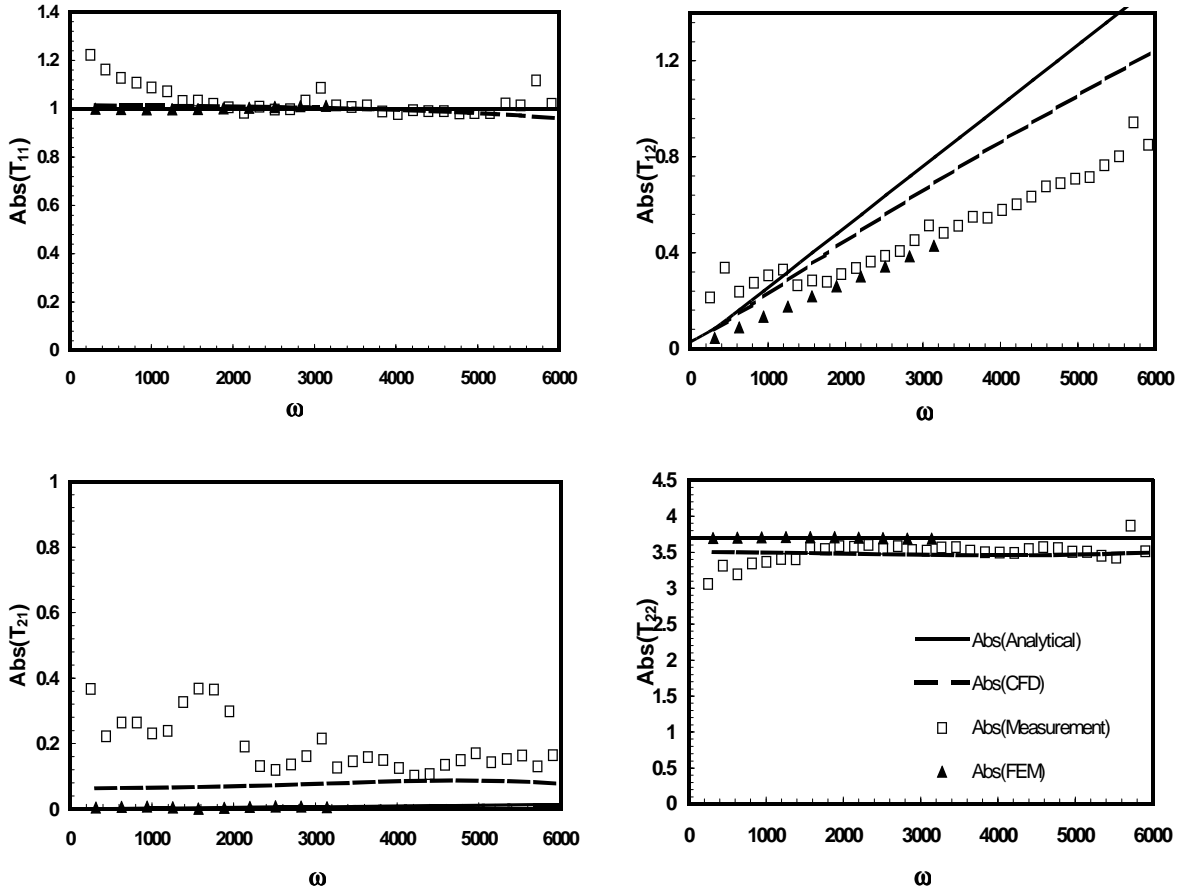


Fig. 4 Absolute Part of Transfer Matrix for a Sudden Change of Tube Width from 0.2m to 0.104m Tube Diameter for an Axisymmetric Duct. Solid Line: Analytical Solution; Dashed Line: CFD; Rectangle: Measurement; Triangle: FEM.

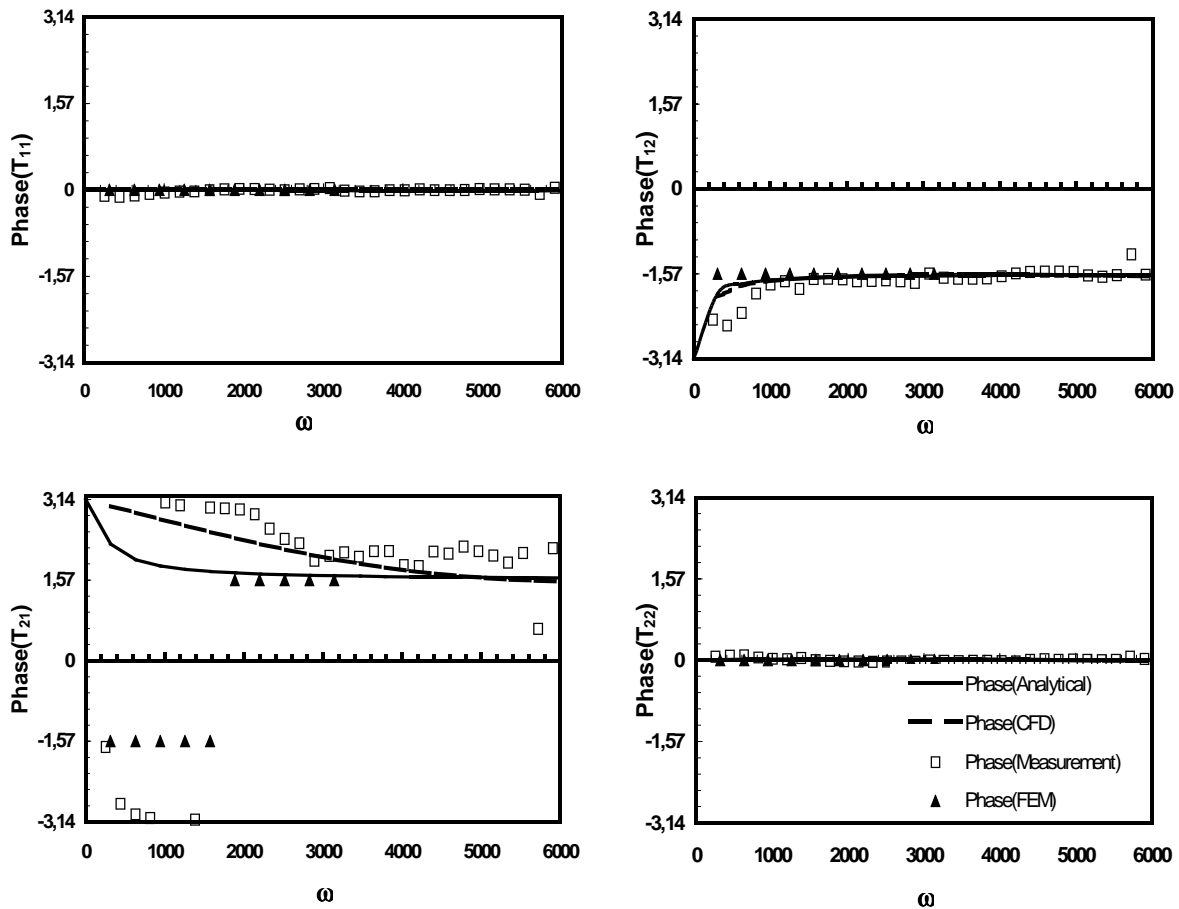


Fig. 5 Phase of Transfer Matrix for a Sudden Change of Tube Width from 0.2m to 0.104m Tube Diameter for an Axisymmetric Duct. Solid Line: Analytical Solution; Dashed Line: CFD; Rectangle: Measurement; Triangle: FEM.

high accuracy for acoustic calculations^{12,15}.

The main differences between the estimated transfer matrices occur for the absolute value in the upper right quadrant (fig. 4). Thus, the leading parameter for the validation of the analytic expression for the transfer matrix of the sudden area change between two pipes, for low Mach number, is the effective length l_{eff} .

The effective length is extracted from the finite element calculations using a linear curve fit for the absolute value of the upper right quadrant of the transfer matrix, see figs. 4 and 6.

4. Results and Validation

The acoustic transfer matrix is estimated for pipes with sudden change of area at Mach numbers below 0.1 and mean flow temperatures of 293K using

CFD/SI.

Fig. 4 and 5 show the absolute value and phase of the transfer matrix for a sudden change of diameter from 0.2m to 0.104m in (pu) notation for a frequency between $\omega = 0$ and about 6000. Solid lines are the analytic solution, dashed lines stand for the CFD/SI result, rectangles represent the measured result, and triangles are the FEM solution, the FEM result is only available up to $\omega = 3000$.

Coefficient T_{11} is the connecting element between pressure up- and downstream of the acoustic element. The analytic solution, the FEM result, and the CFD/SI calculation result show a constant absolute value equal to about 1 for the whole frequency range, whereas the measurement gives values above unity for frequencies below $\omega < 1200$.

The phase (fig. 5) is about zero across the whole frequency range for all four data series.

The differences for the measured result for low frequencies could be accounted towards uncertainties of the measurements, where the microphones used are less accurate.

Coefficient T_{12} shows the relation between acoustic velocity before and acoustic pressure after the acoustic element. The absolute value, both from analysis and FEM show the same gradient. The measured result is different from that below $\omega = 1500$, but good agreement is achieved in comparison to the FEM solution for higher frequencies. CFD/SI and analytical solution predict a slightly higher gradient of the absolute value.

The phase results in a value of $-\pi/2$ above $\omega = 1000$. Below this frequency, the analytical solution increases from $-\pi$ to $-\pi/2$. The FEM result maintains a phase of $-\pi/2$ across the whole frequency. For ω towards zero, Mach number effects become dominant and the phase tends towards $-\pi$, which is not accounted for by the FEM method. The measured result shows a decreased value below $-\pi/2$ with fluctuations.

The differences between the slope of the CFD/SI solution and the analytical result can not be explained simply. They will be discussed in detail below.

Coefficient T_{21} of the transfer matrix represents the connection between acoustic pressure before and acoustic velocity after the acoustic element. The absolute value is predicted to be about 0.07 from the CFD/SI calculation, the measured result shows decreasing tendency from a value of about 0.36 to 0.1 with increasing frequency. The absolute value predicted by FEM is nearly zero, the analytical solution shows a value of about 0.03.

The phase value of the transfer matrix is different for all four results. The analytical solution results in a phase decreasing from π to $\pi/2$. The CFD/SI result decreases from π to a value of about $\pi/2$ over a larger frequency range than the analytical solution. Except for low frequencies, where values from $-\pi/2$ to π were observed, the measured phase follows the CFD/SI result. The FEM calculation results in a phase of $-\pi/2$ below $\omega = 1600$, above this frequency, a value of $\pi/2$ is reported.

Coefficient T_{22} is the connection between acoustic velocity up- and downstream of the acoustic element. The absolute value maintains a value of about 3.7 across the whole frequency range for FEM and the analytical solution. For the measurement data (above $\omega = 1000$) and the CFD/SI result, a slightly lower value of about 3.5 is obtained. Below $\omega = 1000$, the measured absolute value decreases to a value of 3.

The phase of the fourth quadrant shows perfect agreement for all four data series.

The main differences between the measurement and the other three data series for the absolute value was accounted towards the inaccuracy of the microphones at lower frequencies. For $\omega > 2000$, the measured absolute value is only a little larger than the one estimated with CFD/SI. The analytical and FEM result, which neglect

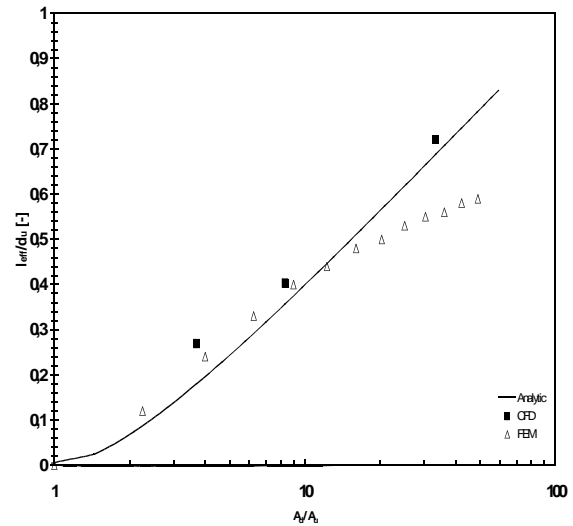


Fig. 6 Effective Length (l_{eff}) as a Function of Area Ratio for Axisymmetric Channels. Solid Line: Analytic Result; Rectangles: CFD Calculation; Triangles: FEM Calculation.

turbulence and mean flow, can not show this effect. Thus, at least part of the difference between the absolute values of CFD/SI (measurement) and analytical (FEM) result can be explained.

Apart from this, the transfer matrices estimated with analytic solution, CFD/SI, measurement, and FEM show high similarity and low fluctuation of the results over frequency. Coefficient T_{11} and T_{22} show almost perfect agreement for all four methods. The main differences are observed for the upper right and lower left quadrants.

In the following, the value for the slope of the absolute value of T_{12} for the acoustic transfer matrix of area changes is examined. This slope is mathematically represented by the term l_{eff} in the analytic expression for the acoustic transfer matrix.

Fig. 6 shows the effective length for area changes with axisymmetric geometry as a function of area ratio for analytical result, CFD/SI and FEM calculation. Comparing CFD/SI and analytical result, the effective length is slightly overestimated from CFD/SI for area ratios between 1 and 33. The FEM solution, on the other hand, shows a value of l_{eff} very close to the other solutions up to area ratios of 10.

Above this value, a decrease is observed for the FEM calculation result. As the result, the three methods show good agreement for a wide range of area ratios.

5. Conclusion

In this paper, a general method for calculating transfer matrices from CFD/SI has been further developed. The method has been applied to the case of a sudden change of cross sectional area between two pipes. It has been validated against finite element computations and an analytical representation.

The application of the CFD-based method to the estimation of acoustic transfer matrices is enhanced by improved boundary excitation. The application of scattering matrix representation leads to further improvement. Therefore, it is concluded that acoustic transfer matrices can be estimated including mean flow and viscous effects with high accuracy.

6. Acknowledgment

The work presented in this paper is supported within the program "AG Turbo II" funded by the Bundesministerium für Wirtschaft und Technologie, Alstom Power, and Siemens AG. Förderkennzeichen: 0327091P. Additional support was granted by Fluent INC.

7. Appendix A

7.1 Mass Conservation

To derive the expression for mass conservation between the upstream plane u and downstream plane d (as used in eq. (11)), the following expression serves as the starting point

$$\frac{d}{dt} \int \rho dV + \int \rho u_i dA_i = 0 \quad (A1)$$

For quasi one-dimensional flow between the two planes u and d , this can be simplified as follows

$$\frac{d}{dt} \int_{x_u}^{x_d} \rho(x) A(x) dx + [\rho u A]_u^d = 0 \quad (A2)$$

For harmonic perturbations with a wave length larger than the length l of the element, $kl = \frac{\omega}{c} l < 1$ and

$\rho'(x) = \rho_u + O(kl)$. It follows that

$$i \omega \rho_u' \int_{x_u}^{x_d} A(x) dx + [(\rho' u + \rho u') A]_u^d = O(kl)^2, \quad (A3)$$

where O denotes the order of the expression.

Dividing by the mean density ρ , which is valid for small M , and introducing a reduced length as in eq. (13), one obtains

$$\left[A \left(\frac{p'}{\rho c} M + u' \right) \right]_u^d + i \frac{\omega}{c} l_{red} A_d \frac{p_u'}{\rho c} \approx 0 \quad (A4)$$

7.2 Momentum Balance

The starting point for the derivation of the momentum balance between two planes u and d up- and downstream of a compact acoustic element is the Bernoulli equation for irrotational, homentropic flow

$$\frac{\partial}{\partial x_i} \left(\frac{\partial \phi}{\partial t} + \frac{u^2}{2} + \frac{y}{\gamma-1} \frac{p}{\rho} \right) = 0 \quad (A5)$$

Integrating this expression along a streamline of the mean flow from x_u to x_d , a coupling relation between the two planes is derived. First consider the first term in eq. (A5), the velocity potential

$$\frac{\partial}{\partial t} \int_{x_u}^{x_d} \frac{\partial \phi}{\partial x_i} dx_i = \frac{\partial}{\partial t} \int_{x_u}^{x_d} u_i dx_i \approx \frac{\partial}{\partial t} u_u \int_{x_u}^{x_d} \frac{A_u}{A(x)} dx \quad (A6)$$

The approximation $u(x) \approx u_c A(x)$ is valid if the flow through the element is essentially incompressible, i.e. if the element is acoustically compact ($kl < 1$), assuming steady mean flow, and harmonic perturbation, an extended length is introduced

$$l_{eff} \equiv \int_{x_u}^{x_d} \frac{A_u}{A(x)} dx, \quad (A7)$$

the following approximation is obtained

$$\frac{\partial}{\partial t} \int_{x_u}^{x_d} \frac{\partial \phi}{\partial x_i} dx_i = i \omega l_{eff} u_u' \quad (A8)$$

The remaining two terms in eq. (A5) are simply evaluated at x_u and x_d . Linearization and dividing by c yields

$$\left[\frac{p'}{\rho c} + M u' \right]_u^d + l_{eff} \frac{i \omega}{c} u_u' + \zeta M_u u_u' = O(kl)^2 \quad (A9)$$

This result is exact to first order in Helmholtz number (kl). The terms of second order in small quantities kl and M are neglected.

8. Appendix B

8.1 Derivation of the Effective Length

To derive the effective length as a function of the analogous impedance L_a , a comparison between the kinetic energy and the expression for the effective length is performed. The kinetic energy due to the area change is obtained by the following expression¹⁴

$$KE = \frac{1}{2} L_a (A_u u_u)^2 \quad (A10)$$

The kinetic energy can also be obtained using the kinetic energy density $\frac{1}{2} \rho u^2$

$$KE = \int_{x_u}^{x_d} \frac{1}{2} \rho u(x)^2 A(x) dx \quad (A11)$$

Since mass conservation yields $u(x)A(x) = U_u A_u$, eq. (A11) can be transformed into

$$KE = \int_{x_u}^{x_d} \frac{1}{2} \rho u_u A_u u(x) dx = \frac{1}{2} \rho u_u A_u \int_{x_u}^{x_d} \frac{u_u A_u}{A(x)} dx \quad (A12)$$

Using the definition of the effective length as in eq. (14), the kinetic energy is obtained as a function of density

$$KE = \frac{1}{2} \rho u_u^2 A_u l_{eff} \quad (A13)$$

Comparison between eqs. A10 and A13 yields the relation between l_{eff} and L_a

$$l_{eff} = \frac{L_a A_u}{\rho} \quad (A14)$$

8.2 Derivation of the Reduced Length

The reduced length is derived from the expression for periodic structures of acoustic elements used by Morse and Ingard¹⁴

$$u_d' = i \frac{\omega}{c} C_a p_u' + (1 - i \omega C_a Z_a) u_u' \quad (A15)$$

where C_a is the analogous capacitance and Z_a the analogous impedance. The analogous capacitance can be expressed by the analogous inductance via the following expression

$$C_a = \frac{1}{L_a c^2} \quad (A16)$$

Introducing eq. (A16) into (A15) and comparing to eq. (15) yields the expression for the reduced length

$$l_{red} = -\frac{\rho}{L_a c} \quad (A17)$$

8.3 Derivation of the Acoustic Loss Coefficient

The acoustic loss coefficient ζ is derived from the expression for periodic structures of acoustic elements used by Morse and Ingard¹⁴

$$p_d' = p_u' - (R_a - i \omega L_a) A_u u_u' \quad (A18)$$

Dividing this by ρc leads to

$$\frac{p_d'}{\rho c} = \frac{p_u'}{\rho c} - \left(\frac{R_a}{\rho c} - i \frac{\omega L_a A_u}{\rho} \right) u_u' \quad (A19)$$

where the first expression in brackets yields the expression for the acoustic loss coefficient by comparison to eq. (15)

$$\zeta = \frac{R_a A_u}{\rho c M_u} \quad (A20)$$

In addition, the second term in brackets leads to an alternative derivation of the effective length.

9. References

1. Polifke, W., Poncet, A., Paschereit, C.O., Döbbling, K., Determination of (Thermo-)Acoustic Transfer Matrices by Time-Dependent Numerical Simulation, 7th Int'l Conference on Numerical Combustion, York, UK, 1998.
2. Polifke, W., Poncet, A., Paschereit, C.O., Döbbling, K., Reconstruction of Acoustic Transfer Matrices by Instationary Computational Fluid Dynamics, J. of Sound and Vibration, 245(3), pp.483-510, 2001.
3. Zhu, M., Dowling, A.P., Bray, K.N.C., Flame Transfer Function Calculation for Combustion Oscillations, Int'l Gas Turbine and Aeroengine Congress & Exhibition, ASME 2001-GT-374, New Orleans, LA, 2001.
4. Polifke, W., Kopitz, J., Serbanovic, A., Impact of the Fuel Time Lag Distribution in Elliptical Premix Nozzles on Combustion Stability, 7th AIAA/CEAS Aeroacoustics Conference, AIAA 2001-2104, Maastricht, NL, 2001.
5. Fluent 6 Documentation, Fluent Inc., Ventera Resource Park, Lebanon, NH, 2002.
6. Müller, B., Low Mach Number Asymptotics of the Navier-Stokes Equations and Numerical Implications, 30th Computational Fluid Dynamics Lecture Series, von Karman Institute for Fluid Mechanics, 1999.
7. Polifke, W., Wall, C. Estimation of (Thermo-)Acoustic Transfer Matrices by Large Eddy Simulation, Center for Turbulence Research, Proceedings of the Summer Program, 2002.
8. Isermann, R., Identifikation dynamischer Systeme 1+2, Springer Verlag, 1992.
9. Ljung, L., System Identification. Theory for the User, PTR Prentice Hall Information and System Series, 1999.
10. Åbom, M., Boden, H., Error analysis of Two-Microphone Measurements in Ducts with Flow, J. Acoustics. Soc. Am., Vol.83 (6), pp. 2429-2438, 1988.
11. Paschereit, C. O., Schuermans, B. B. H., Polifke, W.

- Mattson, O., Measurement of transfer matrices and source terms of premixed flames, *J. Eng. for Gas Turbines and Power*, Vol. 124, pp. 239-247, 2002.
12. Pankiewicz, C., Fischer, A., Hirsch, C., Sattelmayer, T., Computation of Transfer Matrices for Gas Turbine Combustors including Acoustics/Flame Interaction, 9th AIAA/CEAS Aeroacoustics Conference & Exhibit, Hilton Head, 2003.
 13. Munjal, M. L., *Acoustics of Ducts and Mufflers*, Wiley, 1987.
 14. Morse, P.M., Ingard, U.I., *Theoretical Acoustics*, Princeton University Press, 1986.
 15. Peat, K.S., The Acoustical Impedance at Discontinuities of Ducts in the Presence of a Mean Flow, *J. of Sound and Vibration*, 127(1), pp. 123-132, 1988.
 16. Schinzinger, R., Laura, P.A.A., *Conformal Mapping: Methods and Applications*, Elsevier Science Publishers B.V., 1991.
 17. Dupere, I.D.J., Dowling, A.P., The Absorption of Sound near Abrupt Axisymmetric Area Contractions, *J. Of Sound and Vibration*, 239(4), pp. 709-730, 2001.
 18. Polifke, W., Gentemann, A.M.G., Order and Realizability of Impulse Response Filters for Accurate Identification of Acoustic Multi-Ports from Transient CFD, 10th Int. Conf. on Sound and Vibration, Stockholm, Sweden, 2003.
 19. Reynst, F.H., *Pulsating Combustion*, Pergamon Press, 1961.